The ketone body β-hydroxybutyrate ameliorates neurodevelopmental deficits in the GABAergic system of *daf-18/PTEN Caenorhabditis elegans* mutants

Sebastián Giunti[1,2], María Gabriela Blanco[1,2], María José De Rosa[1,2*] and Diego Rayes[1,2*]

1-Instituto de Investigaciones Bioquímicas de Bahía Blanca (INIBIBB) CCT UNS-CONICET, Bahía Blanca, Argentina

2-Departamento de Biología, Bioquímica y Farmacia, Universidad Nacional Del Sur (UNS), Bahía Blanca, Argentina

Correspondence to:

Maria José De Rosa (mjderosa@criba.edu.ar)

Diego Rayes (drayes@criba.edu.ar)

Highlights

***daf-18/PTEN* deficiency in *C. elegans* results in a specific impairment of inhibitory GABAergic signaling, while the excitatory cholinergic signaling remains unaffected.

*The dysfunction of GABAergic neurons in these mutants arises from the inactivity of the transcription factor DAF-16/FOXO during their development, resulting in conspicuous morphological and functional alterations.

*A diet enriched with the ketone body β-hydroxybutyrate induces DAF-16/FOXO activity in *daf-18/PTEN* mutants, therefore mitigating the functional and morphological defects in the development of GABAergic neurons

*β-hydroxybutyrate supplementation during the early stages of development is both necessary and sufficient to achieve these rescuing effects on GABAergic signaling in *daf-18/PTEN* mutants.

Abstract

A finely tuned balance between excitatory and inhibitory signals is essential for proper brain function. Disruptions in the GABAergic system, which alter this equilibrium, are a common feature in various types of neurological disorders, such as Autism Spectrum Disorders (ASD).

Mutations in PTEN, the main negative regulator of the PI3K/Akt pathway, are strongly associated with ASD. However, it is unclear whether PTEN deficiencies can differentially affect inhibitory and excitatory signaling. Using the *C. elegans* neuromuscular system, where both excitatory (cholinergic) and inhibitory (GABAergic) inputs regulate muscle activity, we found that *daf-18*/*PTEN* mutations specifically impact GABAergic (but not cholinergic) neurodevelopment and function. The specific defects observed in the GABAergic system in *daf-18/PTEN* mutants are due to reduced activity of DAF-16/FOXO during development. Ketogenic diets (KGDs) have proven effective for disorders associated with excitatory/inhibitory (E/I) imbalances. However, the mechanisms underlying their action remain elusive. We show, in *daf-18/PTEN* mutants, that a diet enriched with the ketone body β-hydroxybutyrate during early development improves GABAergic neurodevelopment and function in a DAF-16/FOXO-dependent manner. Our study contributes to the universal understanding of the proven link between *PTEN* mutations and neurodevelopmental defects and, more importantly, provides new insights into the mechanisms underlying KGDs' positive effects on neuronal disorders characterized by GABAergic dysfunction.

INTRODUCTION

Maintaining a delicate balance between excitatory and inhibitory (E/I) neurotransmission is critical for optimal brain function [1]. Disruptions in this balance are commonly observed in neurodevelopmental disorders [2-4]. In particular, deficits in inhibitory (GABAergic) signaling have been reported in Autism Spectrum Disorders (ASD) and other related physiopathological conditions [4,5].

PTEN is a classical tumor suppressor gene that antagonizes the highly conserved phosphatidylinositol 3-phosphate kinase (PI3K)/protein kinase B (PKB/Akt) pathway. Several reports using animal models have highlighted the importance of *PTEN* in neurodevelopment [6-12]. Moreover, mutations in *PTEN* were frequently found in human patients presenting ASD [13]. The molecular events underlying the neurodevelopmental deficits in *PTEN* mutants remain poorly understood.

Ketogenic diets (KGDs), which are very high in fat and low in carbohydrates, upregulate beta-oxidation of fatty acids and the release of ketone bodies (KBs), which serve as an energy source for other cells. These diets have been shown to be effective in alleviating autistic symptoms [14-16]. It is mostly unknown how the KGDs exert these beneficial effects.

The *C. elegans* neuromuscular system, where both excitatory (cholinergic) and inhibitory (GABAergic) motor neurons regulate muscle contraction and relaxation, provides an excellent platform for studying the function, balance, and coordination between excitatory and inhibitory signals[17-23]. Studies conducted within this system have yielded valuable insights into fundamental synaptic transmission mechanisms[24,25]. Over the last decade, numerous studies focused on this simple yet highly informative system have significantly contributed to our understanding of the functioning and dysregulation of human genes associated with neurodevelopmental disorders, epilepsy, and familial hemiplegic migraine[17,22,23,26]. Furthermore, the substantial conservation of the main components of the PI3K/Akt pathway in *C. elegans*[27,28], enhances the applicability of this model system for investigating the role of this pathway in neurodevelopment.

Here we find that mutations in *daf-18* (ortholog for *PTEN* in *C. elegans*) lead to selective impairments in GABAergic inhibitory signaling due to reduced activity of the transcription factor DAF-16/FOXO during neurodevelopment. Surprisingly, cholinergic excitatory motor neurons remain unaffected. Even more significantly, we demonstrate that exposure of these animals to a diet enriched with the KB β-hydroxybutyrate (βHB) early during development increases DAF-16 activity, ameliorates morphological and functional defects in GABAergic neurons, and improves behavioral phenotypes. Besides providing a behavioral simple system to study the role of the conserved PI3K/Akt/FOXO pathway in neurodevelopment, this study constitutes a proof of concept of the ability of reverting a neurodevelopmental defect with a dietary intervention and contributes to understanding the mechanisms of action of KBs and their potential therapeutic use.

RESULTS

Disturbances in *C. elegans* cholinergic or GABAergic activity can be detected by analyzing the sensitivity to the paralyzing effects of drugs that exacerbate cholinergic transmission [17,18]. We therefore analyzed the sensitivity of *daf-18* deficient animals to the acetylcholinesterase inhibitor aldicarb and to the cholinergic agonist levamisole. Exposure to aldicarb leads to an increase in ACh levels at cholinergic motor synapses, resulting in massive activation of muscular cholinergic receptors and subsequent paralysis [29]. Levamisole also induces paralysis by directly activating muscular cholinergic receptors [29]. We found that *daf-18* mutants are hypersensitive to the paralyzing effects of both drugs (Figures 1A, 1B and S1D).

Reduced activity of DAF-18 has been largely shown to exacerbate the PI3K pathway, precluding the activation of DAF-16, the *C. elegans* ortholog of the FOXO transcription factors family [28] (Figure S1A). We analyzed aldicarb and levamisole sensitivity of mutants in this transcription factor. Similar to *daf-18* mutants, we found that *daf-16* null mutants are hypersensitive to the paralyzing effects of aldicarb and levamisole (Figures 1A and 1B). Furthermore, we did not observe significant differences in aldicarb and levamisole sensitivity between *daf-18; daf-16*

double null mutants and the respective single mutants, suggesting that both genes affect neuromuscular signaling by acting in the same pathway (Figures 1A and 1B). In addition to *daf-16* and *daf-18*, we assessed the sensitivity to the paralyzing effects of aldicarb and levamisole in mutants of other components of the PI3K pathway, such as *age-1*/PI3K, *pdk-1, akt-1*, and *akt-2* (Figure S1E). We did not observe significant differences compared to the wild-type in most cases, except for the mutant containing the *mg142* allele, which exhibits a gain-of-function mutation in *pdk-1*[27] (all other mutations lead to reduction or complete loss of function mutations in their respective genes). This gain of function mutant displays hypersensitivity to aldicarb and levamisole, similar to *daf-16* and *daf-18* mutants. Given that increased *pdk-1* activity is linked to hyperphosphorylation and inactivation of DAF-16 (Figure S1A), these results support the hypothesis that low activity of DAF-16 leads to hypersensitivity to these drugs. In vertebrates, alterations in PTEN activity have been largely shown to impact neuronal development and function by affecting the mTOR pathway[30]. Consequently, we conducted an analysis to determine whether mutations in components of the *C. elegans* TOR complexes (TORC) would lead to significant changes in sensitivity to aldicarb and levamisole. Our findings indicate that neither animals with loss of the essential TORC1 component *raga-1*/RagA nor animals with a loss of function in the essential TORC2 component *rict-1*/Rictor exhibited significant alterations in sensitivity to cholinergic drugs compared to wild-type animals (Figures S1F). This suggests that the mTOR pathway is not involved in *daf-18* pharmacological phenotypes. Hypersensitivity to cholinergic drugs has long been observed in worms where there is a deficiency in GABAergic signaling [17,18] (Figures 1A and 1B). In mutants with severe deficits in GABA transmission, prodding induces a bilateral contraction of the body wall muscles that shortens the body (shrinker phenotype) [31]. When *daf-18* mutants are touched, there is a slight but significant shortening in body length (Figure 1C). As expected, this shortening is not as noticeable as in animals with a complete deficit in GABAergic signaling, such as mutants in *unc-25* (the *C. elegans* orthologue for glutamic acid decarboxylase) (Figure 1C). Similar to *daf-18* mutants, *daf-16* animals also

exhibit a mild decrease in body length after prodding. Consistent with our aldicarb and levamisole results, there are no significant differences in body shortening between *daf-18; daf-16* double mutants and the corresponding single mutants (Figure 1C), further supporting the notion that both genes act in the same pathway to impact neuromuscular signaling.

We also analyzed other behaviors that require a concerted activity of GABAergic and cholinergic systems, such as the omega turns during the escape response [32]. In *C. elegans* the escape response can be induced by a gentle touch on the head and involves a backward movement that is usually followed by a sharp omega turn and a 180º change in its direction of locomotion [32] (Movie 1). The execution of the omega turn involves a hypercontraction of the ventral muscles and relaxation of the dorsal muscles (see Figure 1D and Movie 1), allowing the animal to make a sharp turn, where the animal's head slides on the ventral side of the body (closed omega turn), and resume locomotion in the opposite direction. In response to anterior touch the vast majority of the wild-type worms make a closed omega turn[32,33]. Ventral muscle contraction is triggered by cholinergic motor neurons (VA and VB neurons) that synapse onto ventral muscles, while dorsal muscle relaxation is induced by GABAergic motor neurons (DD neurons) that synapse onto dorsal muscles (Figure S1C) [32,33]. Ablation of DD GABAergic neurons reduces dorsal muscle relaxation, therefore preventing the head from touching the ventral side of the body during the escape response (open omega turn)[32]. In agreement with previous reports, we found that 93% of wild-type animals exert a closed omega turn within the escape response (Figure 1D). We observed that, similar to wild-type animals, gentle anterior touch with an eyelash induces *daf-18* mutants to move backward and initiate an omega turn (Movie 2). However, only 54% of *daf-18* mutants exhibit the typical head to tail contact during the omega turn (Figure 1D). Akin to *daf-18* mutants, *daf-16* mutants exhibited a decrease in the proportion of closed omega turns (Figure 1D). No additive effects were observed in the *daf-18; daf-16* double mutant, suggesting that the increased inactivation of *daf-16* is primarily responsible for the defects observed in the escape response of *daf-18* mutants.

Given that our results suggest a deficit in GABAergic functionality in *daf-18/PTEN* mutants, we used optogenetics to specifically activate these neurons in mutant worms. This technique has been extensively used in *C. elegans* to study the functionality of the neuromuscular system in intact animals [34-38]. The expression of Channelrhodopsin (ChR2) in GABAergic motor neurons (using the *unc-47* promoter, orthologue for the vesicular GABA transporter SLC32A1) elicits a flaccid paralysis of the worms upon exposure to blue light. This obvious and robust response results in an increase in body length that can be used as a clear readout [35,38,39](Figure 1E and Movie 3). Interestingly, we found that the elongation of the animal after the specific activation of GABAergic neurons is significantly decreased in *daf-18* and *daf-16* mutants compared to wild-type worms (Figure 1E). While these results suggest a defect in GABAergic transmission, it could also be possible that general neuronal transmission is affected. Consequently, we reciprocally activated the cholinergic motor neurons in animals expressing ChR2 under the *unc-17* promoter, which leads to muscle contraction and shortened body length [38,39](Figure 1F and Movie 4). Rather than observing reduced shortening in *daf-16* and *daf-18* mutants, we found that cholinergic activation caused hypercontraction of these mutant animals (Figure 1F). Since the activation of cholinergic motor neurons not only activates muscles but also stimulates GABAergic neurons to produce counteractive muscle relaxation in the other side of the animal (Figure S1C), it is expected that a GABAergic deficit would lead to increased muscle contraction and body shortening upon cholinergic activation. In summary, these results strongly suggest that in *daf-18* and *daf-16* mutants, there is a specific functional defect in GABAergic neurons, while excitatory neurons do not appear to be affected.

Since our previous results imply perturbations of neuromuscular transmission, we explored the morphology of *C. elegans* motor neurons. The cell bodies of both cholinergic (A and B-type) and GABAergic (D-type) motor neurons that innervate body wall muscles are located in the ventral nerve cord (VNC), and a subset extends single process commissures to the dorsal nerve cord (DNC) [40] (Figures 2A, S1C and S2). These commissures allowed us to study defects in the

development or maintenance of GABAergic and cholinergic neuronal processes [41,42]. We analyzed the morphology of GABAergic motor neurons in L4 animals expressing mCherry under the control of the *unc-47* promoter [43]. We found that *daf-18* mutants exhibit a higher frequency of commissure flaws, including guidance defects, ectopic branching, and commissures that fail to reach the dorsal cord (Figures 2B and 2C). GABAergic neuron anomalies were also evident at the first larval stage (L1), suggesting that reduced DAF-18/PTEN activity affects the neurodevelopment of the GABAergic system (Figures 2D and 2E). Since the transcription factor DAF-16/FOXO is one of the main targets of DAF-18/PTEN signaling, we analyzed the morphology of GABAergic D-type neurons in *daf-16* null mutants. These animals also exhibit an increased number of defects in commissures compared to the wild-type (Figure 2C).

Given that *daf-18* is ubiquitously expressed in all tissues [28], we asked whether DAF-18 acts autonomously in GABAergic neurons to ensure proper development. We found that specific *daf-18* expression in GABAergic neurons increased the proportion of closed omega turns in *daf-18* null mutants (Figure 2F). In addition, the morphological defects in GABAergic commissures were significantly reduced (Figure 2G), suggesting that DAF-18 acts autonomously in GABAergic motor neurons to regulate their development.

In contrast to our findings in GABAergic neurons, we observed no obvious differences in the frequency of commissure defects when we compared cholinergic motor neurons in control and *daf-18* animals (Figure S2).

Collectively, our findings demonstrate that mutations in *daf-18* and *daf-16* result in developmental defects in GABAergic neurons, leading to both altered morphology and function, while leaving cholinergic motor neurons unaffected. Our experiments strongly suggest that these specific defects in the inhibitory transmission arises for the hyperactivation of the PI3K pathway, along with subsequent DAF-16 inhibition, in GABAergic neurons of *daf-18/PTEN* mutants.

Mutations in *PTEN* are linked with Autism Spectrum Disorders (ASD) [6]. Ketogenic diets, which force the endogenous production of KBs, have proved to be effective for the treatment of

neurological disorders associated with E/I imbalances, such as epilepsy and, more recently, ASD [14,44,45]. It has been shown that the KB βHB induces DAF-16/FOXO activity [46]. Therefore, we asked whether it is possible to improve the observed phenotypes by modulating the activity of DAF-16 with βHB. We first evaluated the expression of *sod-3*, which codes for a superoxide dismutase and is a DAF-16 transcriptional target gene[47]. We used a strain expressing a GFP transcriptional reporter for *sod-3* and determined fluorescence intensity upon dietary supplementation of βHB. Consistent with previous reports, the levels of SOD-3::GFP are reduced in *daf-18* and *daf-16* mutant strains. Furthermore, we observed that βHB (20 mM) induce the expression of *sod-3* in *daf-18* but not in *daf-16* mutants (Figure S3). Importantly, we did not detect increased *sod-3* expression in *daf-18; daf-16* double deficient animals, strongly suggesting that βHB induces *sod-3* expression in *daf-18* mutants through the transcription factor *daf-16* (Figure S3).

Next, we evaluated behavioral phenotypes and GABAergic neuronal morphology of animals that were raised on an *E. coli* diet supplemented with 20 mM βHB throughout development (from embryogenesis to L4). We found that βHB supplementation significantly reduced the hypersensitivity of *daf-18* mutants to the cholinergic drugs aldicarb and levamisole (Figures 3A and 3B). Moreover, βHB supplementation rescued the post-prodding shortening in *daf-18* mutants (Figure 3C). Accordingly, we found that *daf-18* mutants showed a significant increase in the proportion of closed omega turns during their escape response compared to the naïve condition (Figure 3D). In contrast, βHB exposure does not change the number of closed omega turns in *daf-16* null mutants or the double null mutant *daf-18; daf-16* (Figure 3D).

We subsequently analyzed the changes in body length induced by optogenetic activation of both GABAergic and cholinergic neurons in animals exposed to a diet enriched with βHB. Interestingly, we found that *daf-18* mutants exposed to βHB, but not wild-type or *daf-16* mutant animals, exhibited increased elongation following optogenetic activation of GABAergic neurons (Figures 3F, 3G and 3H). Furthermore, we observed that the hypercontraction observed in *daf-18* mutants

after the activation of cholinergic neurons is significantly reduced in animals exposed to βHB (Figures 3I, 3J and 3K). These findings suggest that this ketone body can rebalance excitatory and inhibitory signals in the *C. elegans* neuromuscular system.

We also evaluated the morphology of GABAergic motor neurons in *daf-18* mutants exposed to βHB. We found that βHB supplementation reduced the frequency of defects in GABAergic processes (Figure 3E). Consistently, βHB exposure did not significantly reduce the defects on GABAergic neurons of either *daf-16* null mutants or *daf-18; daf-16* double mutants. Taken together, these results demonstrate that dietary βHB ameliorates the defects associated with deficient GABAergic signaling in *daf-18* mutants.

It is noteworthy that we did not observe any improvement in either neuronal outgrowth defects in the AIY interneuron or in the migration of the HSN motor neurons (Figure S4) in *daf-18* mutants, even though these defects were shown to depend on the reduction of DAF-16 activity [48,49]. Unlike the development of D-type GABAergic neurons that mainly occurs at L1 larval stages [50], AIY neurite and HSN soma migration take place during embryogenesis [48,51]. It is therefore possible that βHB may not go through the impermeable chitin eggshell of the embryo, as has been reported with other drugs [52].

In the above experiments, βHB was supplemented throughout development: from embryonic stages to the L4 larval stage. We next asked whether there is a critical period during development where the action of βHB is required. We exposed *daf-18* mutant animals to βHB supplemented diets at different periods of development (Figure 4A). Interestingly, we found that exposure to βHB during early development (L1) was sufficient to increase the proportion of *daf-18* mutant animals executing a closed omega turn during the escape response. However, when the animals were exposed to βHB at later juvenile stages (L2-L3 or L3-L4), its ability to enhance the escape response of *daf-18* mutants declined (Figure 4B). Moreover, exposing animals to βHB solely at the L1 stage was enough to reduce morphological defects in the GABAergic motor neurons of

this mutants (Figure 4C). Thus, it is likely that βHB acts at very early stages of development to mitigate neurological defects in *daf-18* mutants.

Taken together, our findings demonstrate that mutations in *daf-18*, the *C. elegans* orthologue of PTEN, lead to specific defects in inhibitory GABAergic neurodevelopment without significantly affecting cholinergic excitatory signals. These GABA-specific deficiencies manifest as altered neuronal morphology, hypersensitivity to cholinergic stimulation, reduced responses to optogenetic GABAergic neuronal activation, mild body shortening following touch stimuli, and deficits in the execution of the omega turn. We have determined that these impairments in GABAergic development result from reduced activity of the FOXO orthologue DAF-16 in *daf-18/PTEN* mutants. Importantly, our study's pivotal finding is that a βHB- enriched diet during early development, robustly mitigates the deleterious effects of *daf-18/PTEN* mutations in GABAergic neurons. This protective effect is critically dependent on the induction of DAF-16 by this ketone body.

DISCUSSION

Mutations in *daf-18/PTEN* are linked to neurodevelopmental defects from worms to mammals[11,48,49]. Moreover, decreased activity of PTEN produces E/I disequilibrium and the development of seizures in mice [7]. The mechanisms underlying this imbalance are not clear. Our results demonstrate that reduced DAF-18/PTEN activity in *C. elegans* generates guidance defects, abnormal branching, incomplete commissural outgrowth and deficient function of inhibitory GABAergic neurons, without affecting the excitatory cholinergic neurons.

daf-18 deficient mutants have a shorter lifespan [53]. One possibility is that the defects in GABAergic processes are due to neurodegeneration associated with premature aging rather than developmental flaws. However, this idea is unlikely given that the neuronal defects are already manifest at the L1 stage. In *C. elegans*, the GABAergic motor neurons rearrange during L1-L2 stages [50,54]. Since the commissures are defective already at the early L1 stage (prior to rewiring),

we can infer that this specific impairment in the neurodevelopment of GABAergic motor neurons is not a consequence of deficient rearrangement during the early larval stages.

Strikingly, cholinergic neurons have no noticeable morphological or functional defects in *daf-18* mutants. Loss-of-function mutants in the neuronal integrin *ina-1,* ortholog of human ITGA6, affect the guidance of GABAergic commissures, without affecting cholinergic neurons [42]. Similar to *PTEN*, mutations in neuronal integrins have been linked to neurodevelopmental defects [55]. Interestingly, the PI3K/Akt/FOXO pathway and integrin signaling are interrelated in mammals [56]. This observation opens the possibility that one of the mechanisms by which *daf-18* mutants have defects in GABAergic neurodevelopment involves integrin expression and/or function. Interestingly, mutations in *eel-1*, the *C. elegans* ortholog of HUWE1, or in subunits of the Anaphase-Promoting Complex (APC), lead to developmental and functional alterations in GABAergic neurons but not in cholinergic neurons[22,57], despite their expression in both neuronal types. This observation suggests the existence of compensatory or redundant mechanisms in cholinergic neurons that may not be present in GABAergic neurons.

In mammals, defects in *PTEN* mutants have been typically related to altered function of the mTOR pathway [8,58,59]. However, our results suggest that, in the *C. elegans* neuromuscular system, decreased activity of DAF-18 affects GABAergic development due to a downregulation of DAF-16/FOXO transcription factor activity. The FOXO family of transcription factors is conserved throughout the animal kingdom [60]. There is increasing evidence demonstrating the key role of this transcription factors family in neurodevelopment [61-63]. Downregulation of FOXO activity early in development reproduces neuropathological features found in ASD patients, i.e., increased brain size and cortical thickness [64,65]. The autonomic activity of DAF-18 and DAF-16 coordinates axonal outgrowth in *C. elegans* AIY interneurons and rat cerebellar granule neurons [48]. On the other hand, DAF-18 and DAF-16 in the hypodermis control neuronal migration of the HSN neuron during development [49]. Our rescue experiments strongly suggest that the PI3K/AKT-1/DAF-16 pathway modulates the development of GABAergic motor neurons by acting autonomously in

these cells. Noteworthy, autonomic DAF-16 activity in GABAergic motor neurons is also key for axonal growth during regeneration [66]. These results further emphasize the importance of DAF-16/FOXO in neuronal development and axonal growth.

In many patients suffering from epilepsy, ketogenic diets can control seizures [44,45]. Furthermore, they can reduce behavioral abnormalities in individuals with ASD [14]. While the mechanisms underlying the clinical effects of ketogenic diets remain unclear, it has been shown that these diets correlate with increased GABA signaling [67-69]. We demonstrate here that dietary supplementation of the ketone body βHB ameliorates morphological and functional defects in GABAergic motor neurons of *daf-18* mutants. This improvement depends on the ability of βHB to induce DAF-16 activation. Although ketone bodies were historically viewed as simple carriers of energy to peripheral tissues during prolonged fasting or exercise, our findings confirm more recent reports showing that βHB also possesses a variety of important signaling functions [70]. We can hypothesize several distinct, non-mutually exclusive models by which βHB can induce DAF-16/FOXO-dependent signaling. βHB directly inhibits mammalian histone deacetylases HDAC1 and HDAC2, increasing histone acetylation at the FOXO3a promoter and inducing the expression of this gene [71]. HDAC1 and HDAC2 play an important role as redundant regulators of neuronal development [72]. Interestingly, in *C. elegans* βHB inhibits the class I HDACs to extend worm lifespan in a DAF-16-dependent manner [46]. Therefore, it is possible that βHB-mediated HDAC inhibition upregulates transcription of DAF-16 counterbalancing hyperactivation of the PI3K pathway in *daf-18/PTEN* mutants. Another potential mechanism for the effect of βHB involves the inhibition of the insulin signaling pathway. In mammals, the administration of βHB downregulates the insulin signaling in muscle [73]. Moreover, several reports have shown that βHB administration reduces phosphorylation and activity of Akt/protein kinase downstream of the insulin receptor [74,75]. In *C. elegans*, inhibition of AKT-1 activates DAF-16 [76]. Although understanding the mechanism behind βHB's action will require further studies, our results demonstrate that this ketone body positively modulates DAF-16/FOXO during neuronal development.

Multiple reports, from *C. elegans* to mammals, suggest that there is a sensitive period, typically early in development, where pharmacological or genetic interventions are more effective in ameliorating the consequences of neurodevelopmental defects [77]. However, recent evidence shows that phenotypes associated with certain neurodevelopmental defects can be ameliorated by interventions during adulthood [78]. Our results show that βHB can rescue the phenotypic defects of *daf-18* mutants only when exposure occurs during an early critical period. The inefficacy of βHB at later stages suggests that the role of DAF-16/FOXO in the maintenance of GABAergic neurons is not as relevant as its role in development.

Since the PI3K/Akt pathway is highly conserved in animals, this study provides universally relevant information on how alterations in this pathway lead to neurodevelopmental defects and the mechanisms underlying the positive effects of ketogenic diets on neuronal disorders characterized by GABA dysfunction and altered E/I ratios.

References

1 Tao, H. W., Li, Y. T. & Zhang, L. I. Formation of excitation-inhibition balance: inhibition listens and changes its tune. *Trends Neurosci* **37**, 528-530, doi:10.1016/j.tins.2014.09.001 (2014).

2 Bozzi, Y., Provenzano, G. & Casarosa, S. Neurobiological bases of autism-epilepsy comorbidity: a focus on excitation/inhibition imbalance. *Eur J Neurosci* **47**, 534-548, doi:10.1111/ejn.13595 (2018).

3 Coghlan, S. *et al.* GABA system dysfunction in autism and related disorders: from synapse to symptoms. *Neurosci Biobehav Rev* **36**, 2044-2055, doi:10.1016/j.neubiorev.2012.07.005 (2012).

4 Oblak, A., Gibbs, T. T. & Blatt, G. J. Decreased GABAA receptors and benzodiazepine binding sites in the anterior cingulate cortex in autism. *Autism Res* **2**, 205-219, doi:10.1002/aur.88 (2009).

5 Gogolla, N. *et al.* Common circuit defect of excitatory-inhibitory balance in mouse models of autism. *J Neurodev Disord* **1**, 172-181, doi:10.1007/s11689-009-9023-x (2009).

6 Rademacher, S. & Eickholt, B. J. PTEN in Autism and Neurodevelopmental Disorders. *Cold Spring Harb Perspect Med* **9**, doi:10.1101/cshperspect.a036780 (2019).

7 van Diepen, M. T. & Eickholt, B. J. Function of PTEN during the formation and maintenance of neuronal circuits in the brain. *Developmental neuroscience* **30**, 59-64, doi:10.1159/000109852 (2008).

8 Kwon, C. H. *et al.* Pten regulates neuronal arborization and social interaction in mice. *Neuron* **50**, 377-388, doi:10.1016/j.neuron.2006.03.023 (2006).

9 Smith, G. D., White, J. & Lugo, J. N. Superimposing Status Epilepticus on Neuron Subset-Specific PTEN Haploinsufficient and Wild Type Mice Results in Long-term Changes in Behavior. *Sci Rep* **6**, 36559, doi:10.1038/srep36559 (2016).

10 Clipperton-Allen, A. E. & Page, D. T. Pten haploinsufficient mice show broad brain overgrowth but selective impairments in autism-relevant behavioral tests. *Hum Mol Genet* **23**, 3490-3505, doi:10.1093/hmg/ddu057 (2014).

11 Chen, Y., Huang, W. C., Sejourne, J., Clipperton-Allen, A. E. & Page, D. T. Pten Mutations Alter Brain Growth Trajectory and Allocation of Cell Types through Elevated beta-Catenin Signaling. *J Neurosci* **35**, 10252-10267, doi:10.1523/JNEUROSCI.5272-14.2015 (2015).

12 Clipperton-Allen, A. E. *et al.* Pten haploinsufficiency causes desynchronized growth of brain areas involved in sensory processing. *iScience* **25**, 103796, doi:10.1016/j.isci.2022.103796 (2022).

13 Butler, M. G. *et al.* Subset of individuals with autism spectrum disorders and extreme macrocephaly associated with germline PTEN tumour suppressor gene mutations. *J Med Genet* **42**, 318-321, doi:10.1136/jmg.2004.024646 (2005).

14 Li, Q., Liang, J., Fu, N., Han, Y. & Qin, J. A Ketogenic Diet and the Treatment of Autism Spectrum Disorder. *Frontiers in pediatrics* **9**, 650624, doi:10.3389/fped.2021.650624 (2021).

15 Castro, K., Baronio, D., Perry, I. S., Riesgo, R. D. S. & Gottfried, C. The effect of ketogenic diet in an animal model of autism induced by prenatal exposure to valproic acid. *Nutritional neuroscience* **20**, 343-350, doi:10.1080/1028415X.2015.1133029 (2017).

16 Verpeut, J. L., DiCicco-Bloom, E. & Bello, N. T. Ketogenic diet exposure during the juvenile period increases social behaviors and forebrain neural activation in adult Engrailed 2 null mice. *Physiol Behav* **161**, 90-98, doi:10.1016/j.physbeh.2016.04.001 (2016).

17 Huang, Y. C. *et al.* Gain-of-function mutations in the UNC-2/CaV2alpha channel lead to excitation-dominant synaptic transmission in Caenorhabditis elegans. *Elife* **8**, doi:10.7554/eLife.45905 (2019).

18 Vashlishan, A. B. *et al.* An RNAi screen identifies genes that regulate GABA synapses. *Neuron* **58**, 346-361, doi:10.1016/j.neuron.2008.02.019 (2008).

19 Zhou, X. & Bessereau, J. L. Molecular Architecture of Genetically-Tractable GABA Synapses in C. elegans. *Front Mol Neurosci* **12**, 304, doi:10.3389/fnmol.2019.00304 (2019).

20 Safdie, G. *et al.* RIC-3 phosphorylation enables dual regulation of excitation and inhibition of Caenorhabditis elegans muscle. *Mol Biol Cell* **27**, 2994-3003, doi:10.1091/mbc.E16-05-0265 (2016).

21 Stawicki, T. M., Zhou, K., Yochem, J., Chen, L. & Jin, Y. TRPM channels modulate epileptic-like convulsions via systemic ion homeostasis. *Current biology : CB* **21**, 883-888, doi:10.1016/j.cub.2011.03.070 (2011).

22 Opperman, K. J. *et al.* The HECT Family Ubiquitin Ligase EEL-1 Regulates Neuronal Function and Development. *Cell Rep* **19**, 822-835, doi:10.1016/j.celrep.2017.04.003 (2017).

23 Giles, A. C. *et al.* A complex containing the O-GlcNAc transferase OGT-1 and the ubiquitin ligase EEL-1 regulates GABA neuron function. *J Biol Chem* **294**, 6843-6856, doi:10.1074/jbc.RA119.007406 (2019).

24 Blazie, S. M. & Jin, Y. Pharming for Genes in Neurotransmission: Combining Chemical and Genetic Approaches in Caenorhabditis elegans. *ACS Chem Neurosci* **9**, 1963-1974, doi:10.1021/acschemneuro.7b00509 (2018).

25 Calahorro, F. & Izquierdo, P. G. The presynaptic machinery at the synapse of C. elegans. *Invertebrate neuroscience : IN* **18**, 4, doi:10.1007/s10158-018-0207-5 (2018).

26 Bessa, C., Maciel, P. & Rodrigues, A. J. Using C. elegans to decipher the cellular and molecular mechanisms underlying neurodevelopmental disorders. *Molecular neurobiology* **48**, 465-489, doi:10.1007/s12035-013-8434-6 (2013).

27 Paradis, S. & Ruvkun, G. Caenorhabditis elegans Akt/PKB transduces insulin receptor-like signals from AGE-1 PI3 kinase to the DAF-16 transcription factor. *Genes Dev* **12**, 2488-2498, doi:10.1101/gad.12.16.2488 (1998).

28 Ogg, S. & Ruvkun, G. The C. elegans PTEN homolog, DAF-18, acts in the insulin receptor-like metabolic signaling pathway. *Molecular cell* **2**, 887-893, doi:10.1016/s1097-2765(00)80303-2 (1998).

29 Mahoney, T. R., Luo, S. & Nonet, M. L. Analysis of synaptic transmission in Caenorhabditis elegans using an aldicarb-sensitivity assay. *Nat Protoc* **1**, 1772-1777, doi:10.1038/nprot.2006.281 (2006).

30 Skelton, P. D., Stan, R. V. & Luikart, B. W. The Role of PTEN in Neurodevelopment. *Mol Neuropsychiatry* **5**, 60-71, doi:10.1159/000504782 (2020).

31 McIntire, S. L., Jorgensen, E., Kaplan, J. & Horvitz, H. R. The GABAergic nervous system of Caenorhabditis elegans. *Nature* **364**, 337-341, doi:10.1038/364337a0 [doi] (1993).

32 Donnelly, J. L. *et al.* Monoaminergic orchestration of motor programs in a complex C. elegans behavior. *PLoS. Biol* **11**, e1001529, doi:10.1371/journal.pbio.1001529 [doi];PBIOLOGY-D-12-03108 [pii] (2013).

33 Pirri, J. K. & Alkema, M. J. The neuroethology of C. elegans escape. *Curr. Opin. Neurobiol* **22**, 187-193, doi:S0959-4388(11)00225-X [pii];10.1016/j.conb.2011.12.007 [doi] (2012).

34 Liewald, J. F. *et al.* Optogenetic analysis of synaptic function. *Nat Methods* **5**, 895-902, doi:10.1038/nmeth.1252 (2008).

35 Schultheis, C., Brauner, M., Liewald, J. F. & Gottschalk, A. Optogenetic analysis of GABAB receptor signaling in Caenorhabditis elegans motor neurons. *J Neurophysiol* **106**, 817-827, doi:10.1152/jn.00578.2010 (2011).

36 Seidenthal, M., Vettkotter, D. & Gottschalk, A. WormRuler: A software to track body length used to characterize a super red-shifted channelrhodopsin in Caenorhabditis elegans. *MicroPubl Biol* **2022**, doi:10.17912/micropub.biology.000607 (2022).

37 Zhang, F. *et al.* Multimodal fast optical interrogation of neural circuitry. *Nature* **446**, 633-639, doi:10.1038/nature05744 (2007).

38 Koopman, M., Janssen, L. & Nollen, E. A. A. An economical and highly adaptable optogenetics system for individual and population-level manipulation of Caenorhabditis elegans. *BMC Biol* **19**, 170, doi:10.1186/s12915-021-01085-2 (2021).

39 Hwang, H. *et al.* Muscle contraction phenotypic analysis enabled by optogenetics reveals functional relationships of sarcomere components in Caenorhabditis elegans. *Sci Rep* **6**, 19900, doi:10.1038/srep19900 (2016).

40 Altun, Z. & Hall, D. Nervous system, general description. *WormAtlas. doi* **10**, 103-116 (2011).

41 Caceres Ide, C., Valmas, N., Hilliard, M. A. & Lu, H. Laterally orienting C. elegans using geometry at microscale for high-throughput visual screens in neurodegeneration and neuronal development studies. *PLoS One* **7**, e35037, doi:10.1371/journal.pone.0035037 (2012).

42 Oliver, D. *et al.* Integrins Have Cell-Type-Specific Roles in the Development of Motor Neuron Connectivity. *J Dev Biol* **7**, doi:10.3390/jdb7030017 (2019).

43 Byrne, A. B. *et al.* Inhibiting poly(ADP-ribosylation) improves axon regeneration. *Elife* **5**, doi:10.7554/eLife.12734 (2016).

44 Neal, E. G. *et al.* The ketogenic diet for the treatment of childhood epilepsy: a randomised controlled trial. *The Lancet. Neurology* **7**, 500-506, doi:10.1016/S1474-4422(08)70092-9 (2008).

45 Lambrechts, D. A. *et al.* A randomized controlled trial of the ketogenic diet in refractory childhood epilepsy. *Acta Neurol Scand* **135**, 231-239, doi:10.1111/ane.12592 (2017).

46 Edwards, C. *et al.* D-beta-hydroxybutyrate extends lifespan in C. elegans. *Aging* **6**, 621-644, doi:10.18632/aging.100683 (2014).

47 De Rosa, M. J. *et al.* The flight response impairs cytoprotective mechanisms by activating the insulin pathway. *Nature* **573**, 135-138, doi:10.1038/s41586-019-1524-5 (2019).
48 Christensen, R., de la Torre-Ubieta, L., Bonni, A. & Colon-Ramos, D. A. A conserved PTEN/FOXO pathway regulates neuronal morphology during C. elegans development. *Development* **138**, 5257-5267, doi:10.1242/dev.069062 (2011).
49 Kennedy, L. M., Pham, S. C. & Grishok, A. Nonautonomous regulation of neuronal migration by insulin signaling, DAF-16/FOXO, and PAK-1. *Cell Rep* **4**, 996-1009, doi:10.1016/j.celrep.2013.07.045 (2013).
50 White, J. G., Albertson, D. G. & Anness, M. A. Connectivity changes in a class of motoneurone during the development of a nematode. *Nature* **271**, 764-766, doi:10.1038/271764a0 (1978).
51 Hedgecock, E. M., Culotti, J. G., Hall, D. H. & Stern, B. D. Genetics of cell and axon migrations in Caenorhabditis elegans. *Development* **100**, 365-382, doi:10.1242/dev.100.3.365 (1987).
52 Sato, K. *et al.* Dynamic regulation of caveolin-1 trafficking in the germ line and embryo of Caenorhabditis elegans. *Mol Biol Cell* **17**, 3085-3094, doi:10.1091/mbc.e06-03-0211 (2006).
53 Mihaylova, V. T., Borland, C. Z., Manjarrez, L., Stern, M. J. & Sun, H. The PTEN tumor suppressor homolog in Caenorhabditis elegans regulates longevity and dauer formation in an insulin receptor-like signaling pathway. *Proc Natl Acad Sci U S A* **96**, 7427-7432, doi:10.1073/pnas.96.13.7427 (1999).
54 Petersen, S. C. *et al.* A transcriptional program promotes remodeling of GABAergic synapses in Caenorhabditis elegans. *J. Neurosci* **31**, 15362-15375, doi:31/43/15362 [pii];10.1523/JNEUROSCI.3181-11.2011 [doi] (2011).
55 Wu, X. & Reddy, D. S. Integrins as receptor targets for neurological disorders. *Pharmacol Ther* **134**, 68-81, doi:10.1016/j.pharmthera.2011.12.008 (2012).
56 Moreno-Layseca, P. & Streuli, C. H. Signalling pathways linking integrins with cell cycle progression. *Matrix Biol* **34**, 144-153, doi:10.1016/j.matbio.2013.10.011 (2014).
57 Kowalski, J. R. *et al.* The Anaphase-Promoting Complex (APC) ubiquitin ligase regulates GABA transmission at the C. elegans neuromuscular junction. *Mol Cell Neurosci* **58**, 62-75, doi:10.1016/j.mcn.2013.12.001 (2014).
58 Cupolillo, D. *et al.* Autistic-Like Traits and Cerebellar Dysfunction in Purkinje Cell PTEN Knock-Out Mice. *Neuropsychopharmacology* **41**, 1457-1466, doi:10.1038/npp.2015.339 (2016).
59 Huang, W. C., Chen, Y. & Page, D. T. Genetic Suppression of mTOR Rescues Synaptic and Social Behavioral Abnormalities in a Mouse Model of Pten Haploinsufficiency. *Autism Res* **12**, 1463-1471, doi:10.1002/aur.2186 (2019).
60 Arden, K. C. FOXO animal models reveal a variety of diverse roles for FOXO transcription factors. *Oncogene* **27**, 2345-2350, doi:10.1038/onc.2008.27 (2008).
61 Santo, E. E. & Paik, J. FOXO in Neural Cells and Diseases of the Nervous System. *Curr Top Dev Biol* **127**, 105-118, doi:10.1016/bs.ctdb.2017.10.002 (2018).
62 McLaughlin, C. N. & Broihier, H. T. Keeping Neurons Young and Foxy: FoxOs Promote Neuronal Plasticity. *Trends Genet* **34**, 65-78, doi:10.1016/j.tig.2017.10.002 (2018).
63 de la Torre-Ubieta, L. *et al.* A FOXO-Pak1 transcriptional pathway controls neuronal polarity. *Genes Dev* **24**, 799-813, doi:10.1101/gad.1880510 (2010).
64 Khundrakpam, B. S., Lewis, J. D., Kostopoulos, P., Carbonell, F. & Evans, A. C. Cortical Thickness Abnormalities in Autism Spectrum Disorders Through Late Childhood, Adolescence, and Adulthood: A Large-Scale MRI Study. *Cereb Cortex* **27**, 1721-1731, doi:10.1093/cercor/bhx038 (2017).
65 Paik, J. H. *et al.* FoxOs cooperatively regulate diverse pathways governing neural stem cell homeostasis. *Cell Stem Cell* **5**, 540-553, doi:10.1016/j.stem.2009.09.013 (2009).

66 Byrne, A. B. *et al.* Insulin/IGF1 signaling inhibits age-dependent axon regeneration. *Neuron* **81**, 561-573, doi:10.1016/j.neuron.2013.11.019 (2014).
67 Cantello, R. *et al.* Ketogenic diet: electrophysiological effects on the normal human cortex. *Epilepsia* **48**, 1756-1763, doi:10.1111/j.1528-1167.2007.01156.x (2007).
68 Calderon, N., Betancourt, L., Hernandez, L. & Rada, P. A ketogenic diet modifies glutamate, gamma-aminobutyric acid and agmatine levels in the hippocampus of rats: A microdialysis study. *Neurosci Lett* **642**, 158-162, doi:10.1016/j.neulet.2017.02.014 (2017).
69 Yudkoff, M., Daikhin, Y., Horyn, O., Nissim, I. & Nissim, I. Ketosis and brain handling of glutamate, glutamine, and GABA. *Epilepsia* **49 Suppl 8**, 73-75, doi:10.1111/j.1528-1167.2008.01841.x (2008).
70 Newman, J. C. & Verdin, E. beta-Hydroxybutyrate: A Signaling Metabolite. *Annu Rev Nutr* **37**, 51-76, doi:10.1146/annurev-nutr-071816-064916 (2017).
71 Shimazu, T. *et al.* Suppression of oxidative stress by beta-hydroxybutyrate, an endogenous histone deacetylase inhibitor. *Science* **339**, 211-214, doi:10.1126/science.1227166 (2013).
72 Park, J., Lee, K., Kim, K. & Yi, S. J. The role of histone modifications: from neurodevelopment to neurodiseases. *Signal Transduct Target Ther* **7**, 217, doi:10.1038/s41392-022-01078-9 (2022).
73 Yamada, T., Zhang, S. J., Westerblad, H. & Katz, A. beta-Hydroxybutyrate inhibits insulin-mediated glucose transport in mouse oxidative muscle. *Am J Physiol Endocrinol Metab* **299**, E364-373, doi:10.1152/ajpendo.00142.2010 (2010).
74 Kim, D. H. *et al.* Anti-inflammatory action of beta-hydroxybutyrate via modulation of PGC-1alpha and FoxO1, mimicking calorie restriction. *Aging* **11**, 1283-1304, doi:10.18632/aging.101838 (2019).
75 McDaniel, S. S., Rensing, N. R., Thio, L. L., Yamada, K. A. & Wong, M. The ketogenic diet inhibits the mammalian target of rapamycin (mTOR) pathway. *Epilepsia* **52**, e7-11, doi:10.1111/j.1528-1167.2011.02981.x (2011).
76 Hertweck, M., Gobel, C. & Baumeister, R. C. elegans SGK-1 is the critical component in the Akt/PKB kinase complex to control stress response and life span. *Dev Cell* **6**, 577-588, doi:10.1016/s1534-5807(04)00095-4 (2004).
77 Meredith, R. M. Sensitive and critical periods during neurotypical and aberrant neurodevelopment: a framework for neurodevelopmental disorders. *Neurosci Biobehav Rev* **50**, 180-188, doi:10.1016/j.neubiorev.2014.12.001 (2015).
78 Kepler, L. D., McDiarmid, T. A. & Rankin, C. H. Rapid assessment of the temporal function and phenotypic reversibility of neurodevelopmental disorder risk genes in Caenorhabditis elegans. *Disease models & mechanisms* **15**, doi:10.1242/dmm.049359 (2022).
79 Blanco, M. G. *et al.* Diisopropylphenyl-imidazole (DII): A new compound that exerts anthelmintic activity through novel molecular mechanisms. *PLoS Negl Trop Dis* **12**, e0007021, doi:10.1371/journal.pntd.0007021 (2018).
80 Andersen, N. *et al.* 1-Mesityl-3-(3-Sulfonatopropyl) Imidazolium Protects Against Oxidative Stress and Delays Proteotoxicity in C. elegans. *Front Pharmacol* **13**, 908696, doi:10.3389/fphar.2022.908696 (2022).

Acknowledgments

Some strains were provided by the CGC, which is funded by NIH Office of Research Infrastructure Programs (P40 OD010440). We thank Mark Alkema, and Alex Byrne for strains. We thank Andrés Garelli, Guillermo Spitzmaul, Gabriela Salvador, Mark Alkema, Inés Carrera and Claire Bénard for helpful discussions. In addition, we would like to acknowledge Ignacio Bergé, Adrian Bizet, Carolina Gomila, Marta Stulhdreher and Carla Chrestía for technical support

Funding

This work was supported by Grants from: 1) Consejo Nacional de Investigaciones Científicas y Técnicas, Argentina to INIBIBB (PUE- N22920170100017CO) and to DR/ MJDR (PIP No. 11220200101606CO). 2) Agencia Nacional de Promoción de la Ciencia y la Tecnología ANPCYT Argentina to DR (PICT 2019-0480 and PICT-2021-I-A-00052) and MJDR (PICT-2017-0566 and PICT-2020-1734) and 3) Universidad Nacional Del Sur to DR (PGI: 24/B291) and MJDR (PGI: 24/B261). The funders had no role in the study design, data collection, and analysis, decision to publish, or preparation of the manuscript.

Conflict of Interest

The authors declare that the research was conducted in the absence of any commercial or financial relationships that could be construed as a potential conflict of interest.

Figures

Figure 1

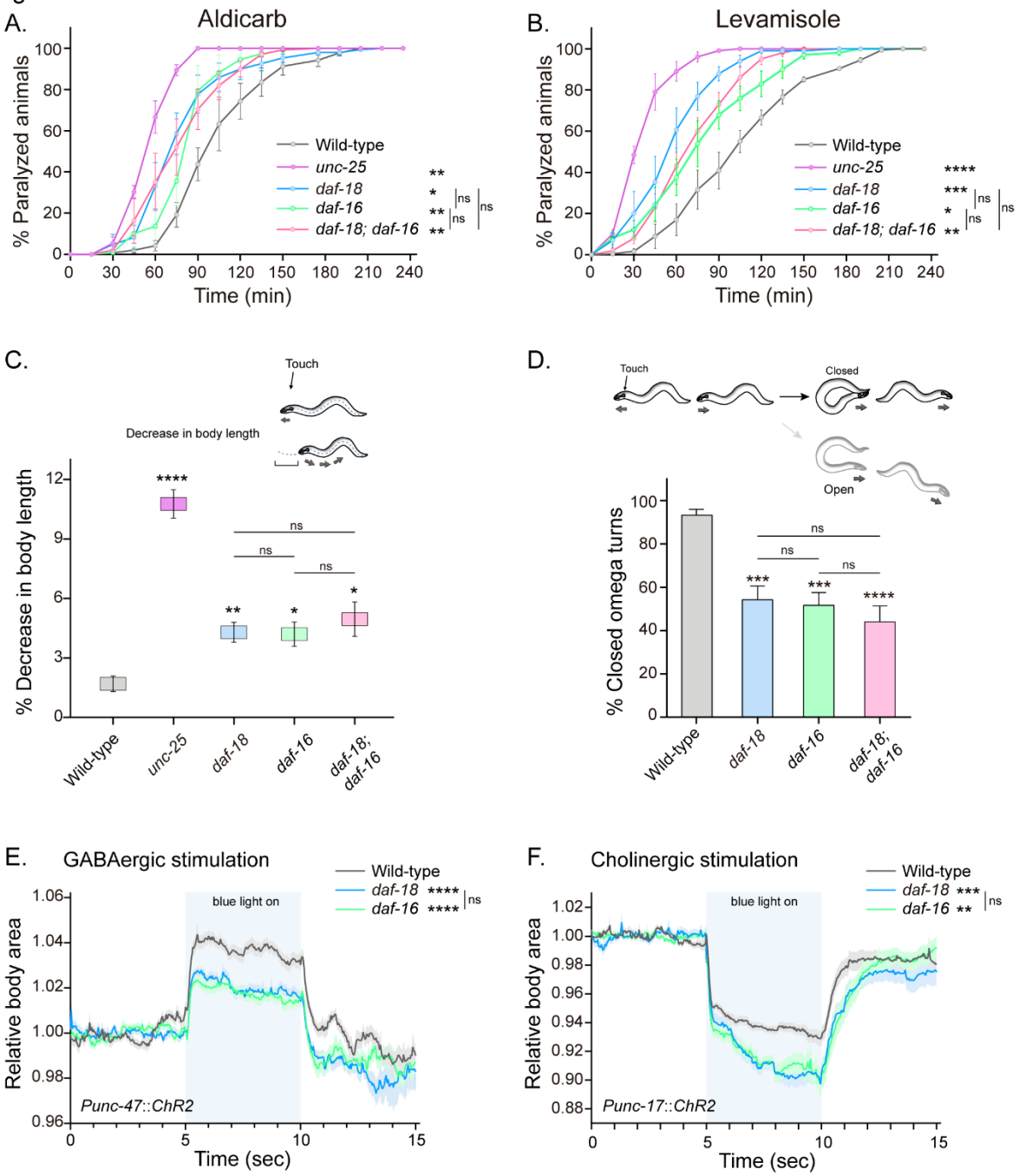

Figure 1. *daf-18/PTEN* mutants exhibit phenotypes typical of GABA-deficient animals. A and B- Quantification of paralysis induced by aldicarb (A) and levamisole (B). At least four independent trials for each condition were performed (n= 25-30 animals per trial). The strain

CB156 *unc-25(e156)* was included as a strong GABA-deficient control. C- Quantification of body shortening in response to anterior touch. Data are represented as mean ± SEM. At least four independent trials for each condition were performed (n= 10-20 animals per genotype/trial). D- (Top) Scheme of *C. elegans* escape response in NGM agar. After eliciting the escape response by an anterior gentle touch, the omega turns were classified as closed (head and tail are in contact) or open (no contact between head and tail). (Bottom) Quantification of % closed omega turns/ total omega turns. At least eight independent trials for each condition were performed (n= 20-25 animals per genotype/trial). E and F- Light-evoked elongation/contraction of animals expressing Channelrhodopsin (*ChR2)* in GABAergic (E) and cholinergic (F) motorneurons. Animals were filmed before, during and after a 5 second-pulse 470nm light stimulus (15 frames/s). The body area in each frame was automatically tracked using a custom FIJI-Image J macro. The averaged area of each animal during the first 125 frames (0-5 seg) established a baseline for normalizing light-induced body area changes. The mean body area during the light pulse was averaged and compared, to analyze statistically significant differences (n=40-55 animals per genotype). Changes in the worm area reflect changes in body length, since the width do not change (see methods and Fig.S1G). Results are presented as mean ± SEM. One-way ANOVA was used to test statistical differences in A, B, D, F and Kruskal-Wallis test was used in C and G (ns $p > 0.05$; * $p \leq 0.05$; ** $p \leq 0.01$; *** $p \leq 0.001$; **** $p \leq 0.0001$).

Figure 2

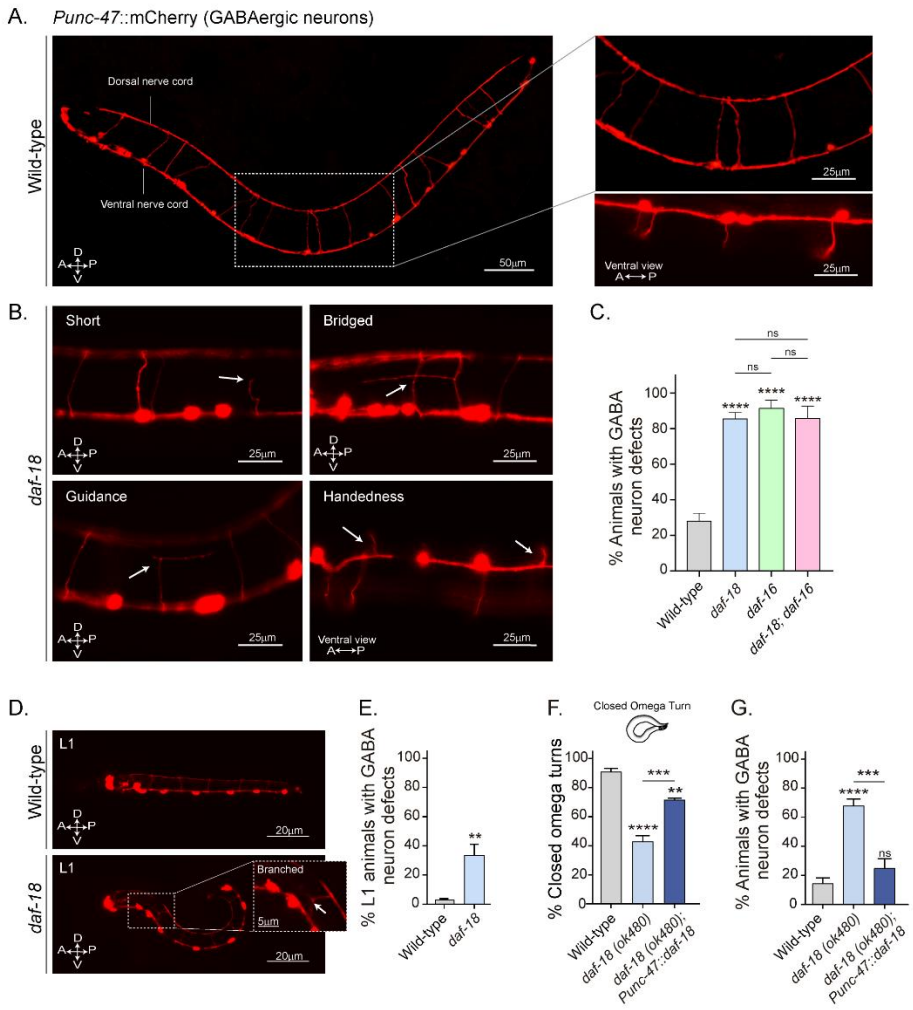

Figure 2. *daf-18/PTEN* mutants show neurodevelopmental defects in GABAergic motor - neurons.

A- Representative image of a wild-type animal expressing mCherry in the GABAergic motor neurons. In the upper inset, commissures are shown at higher resolution. The lower inset shows a ventral view of the animal (all the processes travel through the right side of the animal body).

B- Representative images of commissure defects observed in *daf-18 (ok480)* mutants (arrows). The defects shown are: Short, commissure length less than half of nematode width; Bridged, neighboring commissures linked by a neurite; Guidance, commissures that do not reach dorsal nerve cord; and Handedness, commissure running along the opposite side of the animal's body.

C- Quantification of GABAergic system defects. Each bar represents the mean ± SEM. One-way ANOVA (ns $p > 0.05$; **** $p \leq 0.0001$). At least four independent trials for each condition were performed (n: 20-25 animals per genotype/trial). D- Representative image of L1 animals expressing *Punc-47::mCherry* in wild-type (Top) and *daf-18(ok480)* mutant (Bottom) backgrounds. In this larval stage, only six GABAergic DD motor neurons are born. The inset shows a typical defective (branched) commissure. E- Quantification of GABAergic system defects in L1s. Each bar represents the mean ± SEM. Two-tailed unpaired Student's t test. (**$p \leq 0.01$). At least three independent trials for each condition were performed (n: ~20 animals per genotype/trial). F and G- Quantification of closed omega turns/total omega turns and commissure defects in GABAergic neurons of animals expressing *daf-18* solely in GABAergic neurons. One-way ANOVA (ns $p > 0.05$; **$p \leq 0.01$; *** $p \leq 0.001$; **** $p \leq 0.0001$). At least four independent trials for each condition were performed (n: 15-20 animals per genotype/trial)
A-Anterior; P-Posterior; D-Dorsal; V-Ventral.

Figure 3

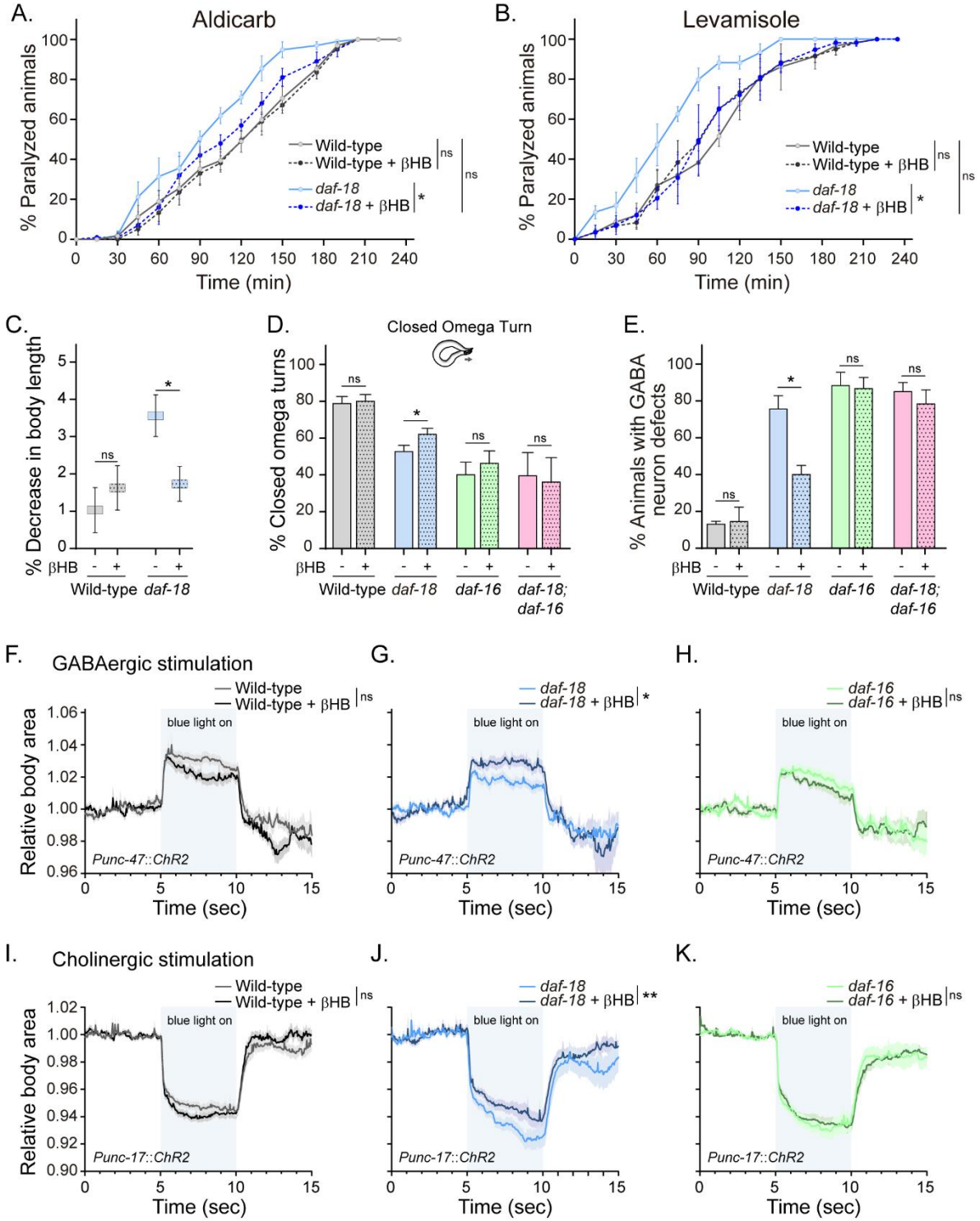
A.
Aldicarb
% Paralyzed animals
Time (min)
Wild-type
Wild-type + βHB
daf-18
daf-18 + βHB
ns
*
B.
Levamisole
C.
% Decrease in body length
βHB
Wild-type
daf-18
D.
Closed Omega Turn
% Closed omega turns
daf-16
daf-18; daf-16
E.
% Animals with GABA neuron defects
F.
GABAergic stimulation
blue light on
Relative body area
Punc-47::ChR2
Time (sec)
G.
H.
daf-16
daf-16 + βHB
I.
Cholinergic stimulation
Punc-17::ChR2
J.
**
K.

Figure 3. Dietary βHB supplementation rescues GABAergic deficits in *daf-18/PTEN* mutants.

Animals were exposed to βHB (20 mM) throughout development (from embryo to L4). A and B- Quantification of paralysis induced by cholinergic drugs. At least four independent trials for each condition were performed (n: 20-25 animals per genotype/trial). C- Measurement of body length in response to anterior touch. Kruskal-Wallis test (ns $p > 0.05$; * $p \leq 0.05$). At least three independent trials for each condition were performed (n= 10-13 animals per genotype/trial). D- Quantification of closed omega turns/total omega turns during the escape response. At least six independent trials for each condition were performed (n= 20 animals per genotype/trial). E- Quantification of commissure defects in GABAergic neurons. Results are presented as mean ± SEM. Two-tailed unpaired Student's t test (ns $p > 0.05$; *$p \leq 0.05$). At least three independent trials for each condition were performed (n= ~20 animals per genotype/trial). F-K- Light-evoked elongation/contraction of animals expressing ChR2 in GABAergic (F-H) and cholinergic (I-K) motorneurons. The mean body area during the light pulse was averaged and compared, to analyze statistically significant differences between treated and not treated groups in each genotype (n=25-35 animals per condition). Two-tailed unpaired Student's t test (ns $p > 0.05$; *$p \leq 0.05$; ** $p \leq 0.01$).

Figure 4

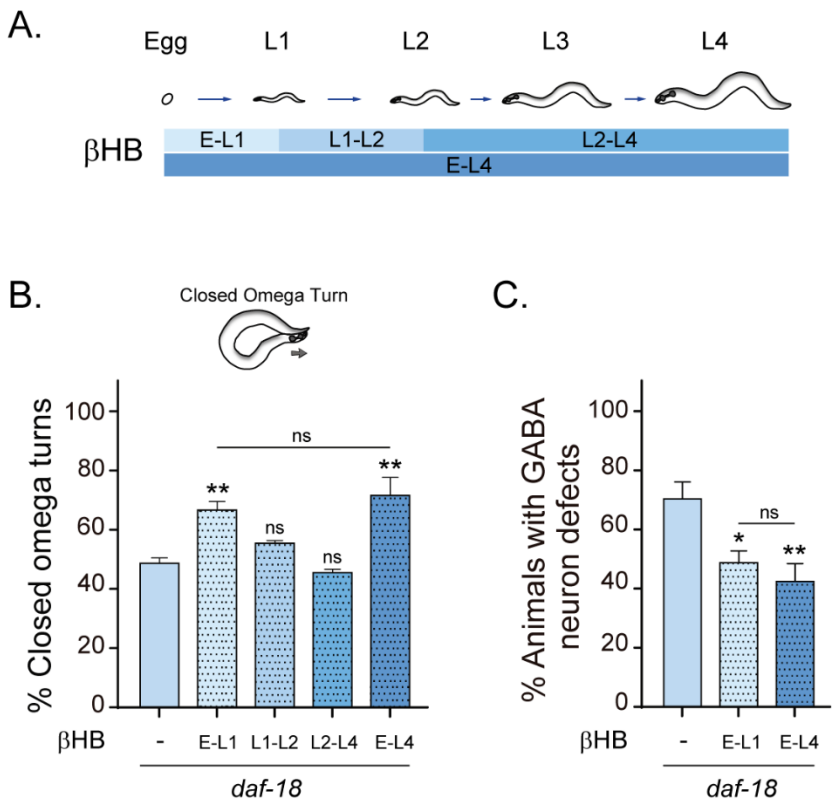

Figure 4. Early developmental stages are critical for βHB-modulation of GABAergic signaling.

A- Animals were exposed to βHB-enriched diet during different developmental intervals: from embryo to the L1 stage (E-L1), from L1 to L2 (L1-L2), from L2 to L4 (L2-L4), or throughout development (from embryo to L4, E-L4). B and C- Quantification of closed omega turns/total omega turns. and GABAergic commissure defects in *daf-18* mutants exposed to βHB at different developmental intervals. Four and six independent trials for each condition were performed in B and C, respectively (n=20-30 (n: 20-25 animals per genotype/trial). Results are presented as mean ± SEM. One-way ANOVA (ns $p > 0.05$; *$p \leq 0.05$; ** $p \leq 0.01$).

Graphical abstract

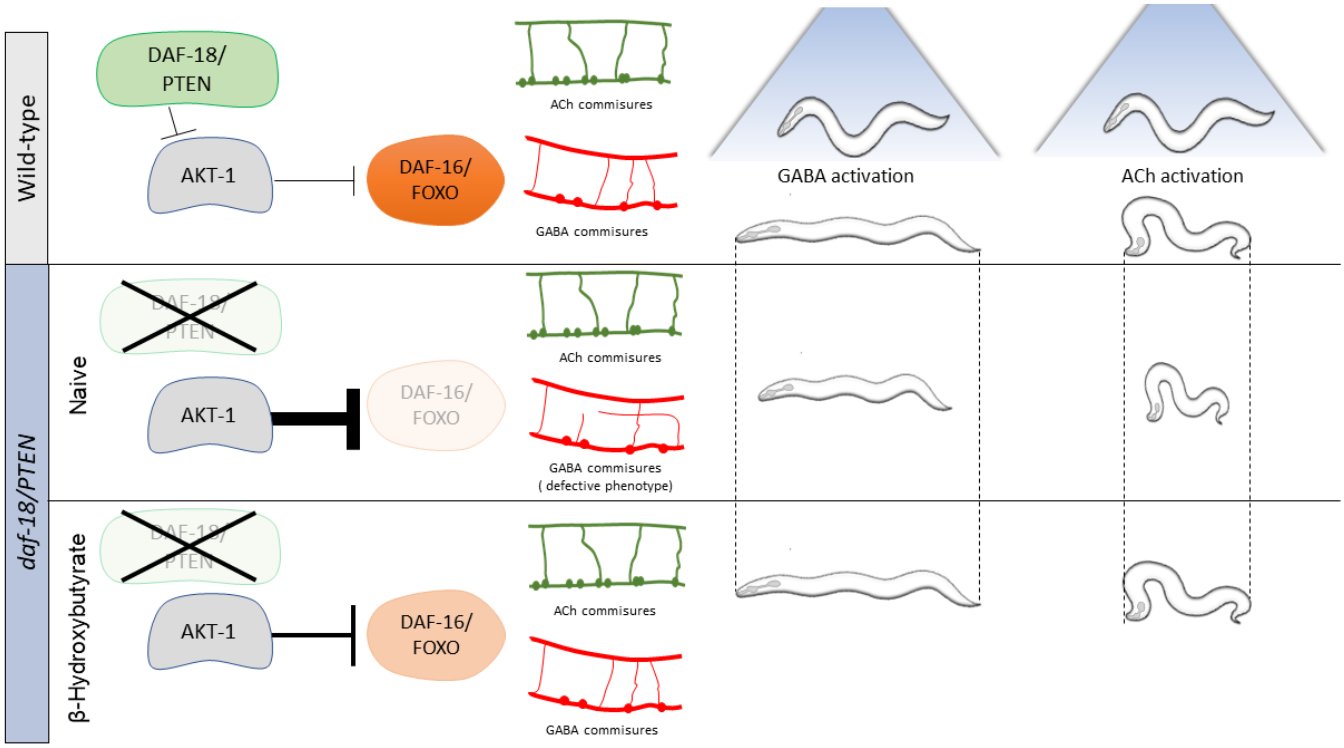

Materials and methods

***C. elegans* culture and maintenance.** All *C. elegans* strains were grown at room temperature (20ºC) on nematode growth media (NGM) agar plates with OP50 *Escherichia coli* as a food source. The wild-type reference strain used in this study is N2 Bristol. Some of the strains were obtained through the *Caenorhabditis* Genetics Center (CGC, University of Minnesota). Worm population density was maintained low throughout their development and during the assays.

Transgenic strains were generated by microinjection of plasmid DNA containing the construct *Punc-47::daf-18cDNA* (kindly provided by Alexandra Byrne, UMASS Chan Medical School) at 20 ng/µL into the germ line of (*daf-18 (ok480); lin-15 (n765ts*)) double mutants with the co-injection marker *lin-15* rescuing plasmid pL15EK (80 ng/µl). At least three independent transgenic lines were obtained. Data are shown from a single representative line.

The strains used in this manuscript were:

CB156 *unc-25(e156*) III

MT6201 *unc-47(n2409*) III

CB1375 *daf-18(e1375*) IV

OAR144 *daf-18(ok480*) IV

GR1307 *daf-16(mgdf50)* I

OAR115 *daf-16(mgDf50); daf-18(ok480)*

OAR161 *daf-18(ok480)*; *Punc-47::daf-18*

LX929 *vsIs48 (Punc-17::gfp)*

IZ629 *ufIs34 (Punc-47::mCherry)*

OAR117 *ufis34 (Punc-47::mCherry); daf-18(ok480)*

OAR118 *vsIs48 (Punc-17::gfp); daf-18(ok480)*

OAR142 *ufis34 (Punc-47::mCherry); daf-16(mgDf50)*

OAR143 *ufis34 (Punc-47::mCherry); daf-16(mgDf50); daf-18(ok480)*

CF1553 *muIs84 [(pAD76) Psod-3::gfp + rol-6(su1006)]*

OAR140 *muIs84 [(pAD76) Psod-3::gfp + rol-6]; daf-18(ok480)*

OAR141 *muIs84 [(pAD76) Psod-3::gfp + rol-6]; daf-16(mgDf50)*

OH99 *mgIS18[Pttx-3::gfp]*

OAR83 *daf-18(ok480); mgIS18[Pttx-3::gfp]*

MT13471 *[Ptph-1::gfp]*

OAR112 *[Ptph-1::gfp]; daf-18(ok480)*

IZ805 *[P*unc-17::ChR2*]*

ZM3266 *[*Punc-47::ChR2*]*

OAR177 *[P*unc-17::ChR2*]; daf-18(ok480)*

OAR178 *[P*unc-17::ChR2*]; daf-16(mgDf50)*

OAR179 *[P*unc-47::ChR2*]; daf-18(ok480)*

OAR180 *[P*unc-17::ChR2*]; daf-16(mgDf50)*

TJ1052 *age-1(hx546)*

GR1310 *akt-1(mg144)*

GR1318 *pdk-1(mg142)*

JT9609 *pdk-1(sa680)*

VC204 *akt-2(ok393)*

VC222 raga-1(ok386)

KQ1366 *rict-1(ft7)*

Paralysis assays. Paralysis assays were carried out in standard NGM plates with 2 mM aldicarb (Sigma-Aldrich) or 0.5 mM levamisole (Alfa Aesar). 25-30 L4 worms were transferred to each plate and paralyzed animals were counted every 15 or 30 minutes. An animal was considered as paralyzed when it did not respond after prodding three times with a platinum wire on the head and tail [79]. At least four independent trials with 25-30 animals for each condition were performed. The

area under the curve (AUC) for each condition in each experiment was used for statistical comparisons

Escape response. Escape response assays were performed on NGM agar plates seeded with a thin bacterial lawn of OP50 *E. coli.* To maintain tight control of growth and moisture, 120 μL of bacteria were seeded 24 hours before the assay and grown overnight at 37º C. The day of the assay, L4 worms were transferred to the plates and allowed to acclimate for at least 5 min. Omega turns were induced by gentle anterior touch with fine eyebrow hair and were classified as closed when the worm touched the tail with its head as previously described [32]. Between 4 and 7 independent trials with ~20 animals for each condition were performed.

Body length assays. Body length measurements were performed in standard NGM agar plates without bacteria. L4 synchronized worms were transferred into the plates and allowed to acclimate for at least 5 min. Worms were recorded with an Amscope Mu300 camera. Animal body length, before and after touching with a platinum pick, was measured using FIJI Image J software. Quantification of body shortening after touching was calculated as the decrease of body length related to the length of the animal before being touched.

Commissure analysis. Synchronized L1 or L4 animals carrying the fluorescence reporters *vsIs48* (*Punc-17::GFP*, cholinergic neurons) or *ufIs34* (*Punc-47::mCherry*, GABAergic neurons) were immobilized with sodium azide (0.25 M) on 2% agarose pads. Commissures of GABAergic and cholinergic neurons were scored with a Nikon Eclipse TE 2000 fluorescence microscope. A commissure is generally composed of a single process, and occasionally two neurites that extend together dorsally. Defects on commissures, including guidance defects, abnormal branching, and incomplete commissures were classified similarly to previous reports [42]. The percentage of animals with at least one commissure defect was calculated for each neuronal class (e.g., cholinergic or GABAergic). At least three trials (~20 animals per condition in each trial) were analyzed for each individual experiment. Representative images shown in the figures were

collected using laser confocal microscopy (ZEISS LSM 900 with AirScan II) with 20× and 63× objectives.

β-hydroxybutyrate assays. Worms were exposed to 20 mM DL-3-hydroxybutyric acid sodium salt (Acros Organics) in NGM agar plates seeded with *E. coli OP50*. Exposure time varied in each trial as indicated (See Figure 4).

***sod-3* expression.** *sod-3* expression levels were analyzed in transgenic strains containing the transcriptional reporter *muIs84*, as described previously [47,80]. Synchronized L4 animals were anesthetized with Sodium Azide (0.25 M) and mounted on 2% agarose pads. Images were collected using a Nikon Eclipse TE 2000 fluorescence microscope. GFP fluorescence intensity was quantified in same-sized ROIs at the head of the animal using Image J FIJI software. Results were normalized to control conditions (wild-type individuals without βHB). ~40-60 animals for each genotype/condition were analyzed.

Optogenetic assays. We examined young adult animals (6-8 hours post-L4 stage) that express Channelrhodopsin (ChR2) in either GABAergic (*Punc-47::ChR2*) or cholinergic neurons (*Punc-17::ChR2*). We transferred these animals to a NGM 6mm agar plate without food, let them acclimate for 5 minutes, and recorded each animal at 15 frames per second using an Allied Vision Alvium 1800 U-500m camera. To stimulate neuronal activity, we exposed the animals to 470 nm light pulses for 5 seconds. These light pulses were delivered using a custom Python script (VIMBA Peron) to an Arduino Uno microcontroller, which operated a Mightex compact universal LED controller (Mightex SLC-MA02-U). The light emission was achieved through a Mightex High-Power LED Collimator Source (LCS-0470–03-11). To precisely track the changes in the worm's body, we continuously monitored its area from 5 seconds before the light stimulus, during the light stimulus and until 5 seconds afterward. We developed a FIJI-Image J macro capable of automatically tracking the body area in each frame, capitalizing on the clear contrast between the worm's body and the background. As demonstrated in Movies 3 and 4, changes in body area

directly corresponded to alterations in the animal's length. To validate our measurement system, we manually measured the width of 6-8 animals at the 2.5-second point of light stimulation and compared them to the body area and length. Our observations consistently showed that, regardless of whether the area increased or decreased (depending on the activation of GABAergic or cholinergic neurons), the width remained mostly unchanged (Fig. S1G). Therefore, the observed changes in the animal´s area measured by our FIJI-Image J macro indeed represent alterations in the animal's length

AIY and HSN analysis. Synchronized L4 or Young Adult worms carrying the fluorescence reporters *Pttx-3::gfp* (AIY interneurons expressing GFP) and *Ptph-1::gfp* (HSN expressing GFP) were immobilized with sodium azide (0.25 M) on 2% agarose pads and analyzed with a Nikon Eclipse TE 2000 fluorescence microscope. AIY neurons morphology were sorted in qualitative categories (see figure legend) while the migration of HSN was classified in quantitative categories using ImageJ software.

Statistical Analysis. The results presented in each figure are the average of at least three independent assays. Bars represent mean ± SEM. Comparison between two groups was carried out using Student's *t*-test, while differences among more than two groups were carried out by One-way analysis of variance (ANOVA). ns $p > 0.05$; * $p \leq 0.05$; ** $p \leq 0.01$; *** $p \leq 0.001$; **** $p \leq 0.0001$. We used the software GraphPad Prism version 6.01 to perform statistics. Other statistical information is indicated in the figure legends. For all assays, the scoring was done blinded.

References

1 Blanco, M. G. *et al.* Diisopropylphenyl-imidazole (DII): A new compound that exerts anthelmintic activity through novel molecular mechanisms. *PLoS Negl Trop Dis* **12**, e0007021, doi:10.1371/journal.pntd.0007021 (2018).

2 Donnelly, J. L. *et al.* Monoaminergic orchestration of motor programs in a complex C. elegans behavior. *PLoS. Biol* **11**, e1001529, doi:10.1371/journal.pbio.1001529 [doi];PBIOLOGY-D-12-03108 [pii] (2013).

3 Oliver, D. *et al.* Integrins Have Cell-Type-Specific Roles in the Development of Motor Neuron Connectivity. *J Dev Biol* **7**, doi:10.3390/jdb7030017 (2019).

4 De Rosa, M. J. *et al.* The flight response impairs cytoprotective mechanisms by activating the insulin pathway. *Nature* **573**, 135-138, doi:10.1038/s41586-019-1524-5 (2019).

5 Andersen, N. *et al.* 1-Mesityl-3-(3-Sulfonatopropyl) Imidazolium Protects Against Oxidative Stress and Delays Proteotoxicity in C. elegans. *Front Pharmacol* **13**, 908696, doi:10.3389/fphar.2022.908696 (2022).

Supplementary Figure

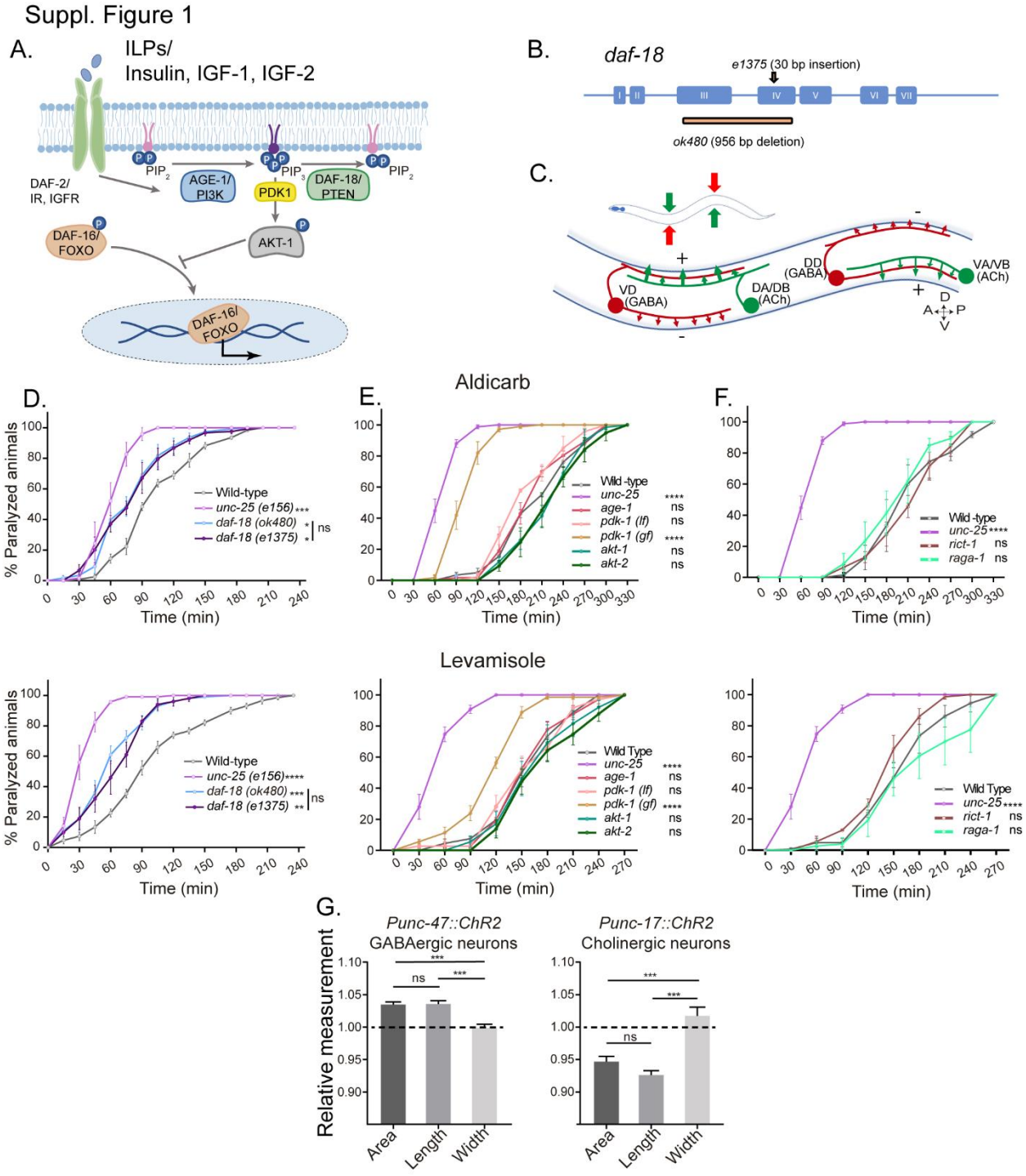

Suppl. Figure 1. *daf-18/PTEN* mutants are hypersensitive to cholinergic drugs.

A- *daf-18/PTEN* encodes a lipid and protein phosphatase that hydrolyzes phosphatidylinositol

(3,4,5)-trisphosphate (PIP_3) to phosphatidylinositol-4,5-bisphosphate (PIP_2). It is the main negative modulator of PDK and AKT activity. In *daf-18/PTEN* mutants, AKT-1 is overactivated leading to high levels of DAF-16/FOXO phosphorylation that prevents the translocation of this transcription factor to the nucleus. B- Gene structure of *daf-18*. Coding sequences are represented by blue boxes. The *daf-18(e1375)* mutant allele inserts a 30 bp sequence in exon IV. This insertion occurs downstream of the phosphatase catalytic domain and causes a frameshift that leads to premature truncation of the protein. This *e1375* mutation partially reduces DAF-18 function. The *daf-18(ok480)* allele contains a 956 bp deletion that removes most of exon 3 and exon 4 and is generally considered to be a null allele. C- Schematic of *C. elegans* neuromuscular circuit. Red indicates GABAergic motor neurons (DD/VD) and green indicates cholinergic motor neurons (VA/VB and DA/DB). The VA and VB cholinergic motor neurons send synaptic inputs to the ventral body wall muscles and to the DD GABAergic motor neurons. The release of ACh from VA/VB neurons leads to the contraction of the ventral body wall muscles and the activation of DD GABAergic motor neurons that release GABA on the opposite side of the worm, causing relaxation of the dorsal body wall muscles. Conversely, activation of the DA and DB cholinergic motor neurons produces contraction of the dorsal body wall muscles and activates the VD GABAergic motor neurons. The VD GABAergic motor neurons release GABA, causing relaxation of the ventral body wall muscles, and thus contralateral inhibition. D-F Quantification of paralysis induced by cholinergic drugs. The assays were performed in NGM plates containing 2 mM aldicarb and 0.5 mM levamisole. Each data point represents the mean percentage of animals paralyzed ± SEM . At least four independent trials with 25-30 animals for each genotype were performed. One-way analysis of variance (ANOVA) was used to test statistical differences among strains (ns $p > 0.05$; * $p \leq 0.05$; ** $p \leq 0.01$; *** $p \leq 0.001$; **** $p \leq 0.0001$). Strains tested are: N2 (wild-type), OAR 144 *daf-18(ok480*), CB1375 *daf-18(e1375*), GR1310 *akt-1(mg144),* TJ1052 *age-1(hx546)*, VC204 *akt-2(ok393), VC222 raga-1(ok386) and* KQ1366 *rict-1(ft7)*. All of these strains carry loss-of-function

mutations. Furthermore, the strains denoted as "*pdk-1* (*lf*)" and "(*gf*)" correspond to JT9609 *pdk-1(sa680)*, which possesses a loss-of-function mutation, and GR1318 *pdk-1(mg142),* which harbors a gain-of-function mutation in the *pdk-1* gene, respectively. The strain CB156 *unc-25(e156)* was included as a strong GABA-deficient control. G- Manual Measurement of Body length and width upon Optogenetic Stimulation of GABAergic (Left) and Cholinergic (Right) neurons. At the 2.5-second time point of light stimulation, we manually measured both the width and length of multiple animals and compared these measurements with the corresponding areas obtained from automated analysis (see Materials and Methods). The width of the worms remained relatively constant, highlighting that the alterations in body area primarily stem from changes in the animal's length

Suppl. Figure 2

A. *punc-17*::GFP (Cholinergic neurons)

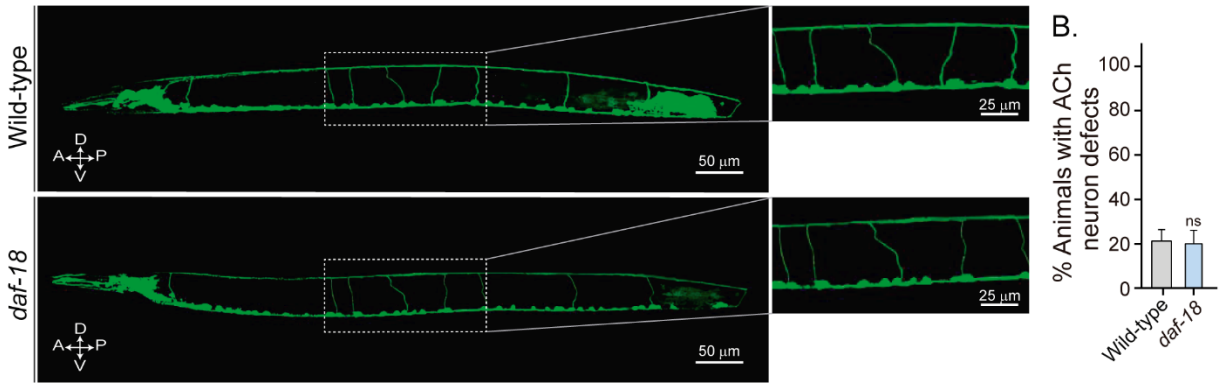

Suppl. Figure 2. *daf-18/PTEN* mutations do not affect excitatory cholinergic motor-neuron morphology

A- Representative images of animals expressing GFP in the cholinergic neurons. In the insets, the commissural processes can be appreciated with higher resolution. B- Quantification of cholinergic system defects. Each bar represents the mean ± SEM for at least four trials (~ 20 animals per trial). Statistical significance between the strains was determined by two-tailed unpaired Student's t test. (ns $p > 0.05$).

A anterior; P Posterior; D Dorsal; V Ventral.

Suppl. Figure 3

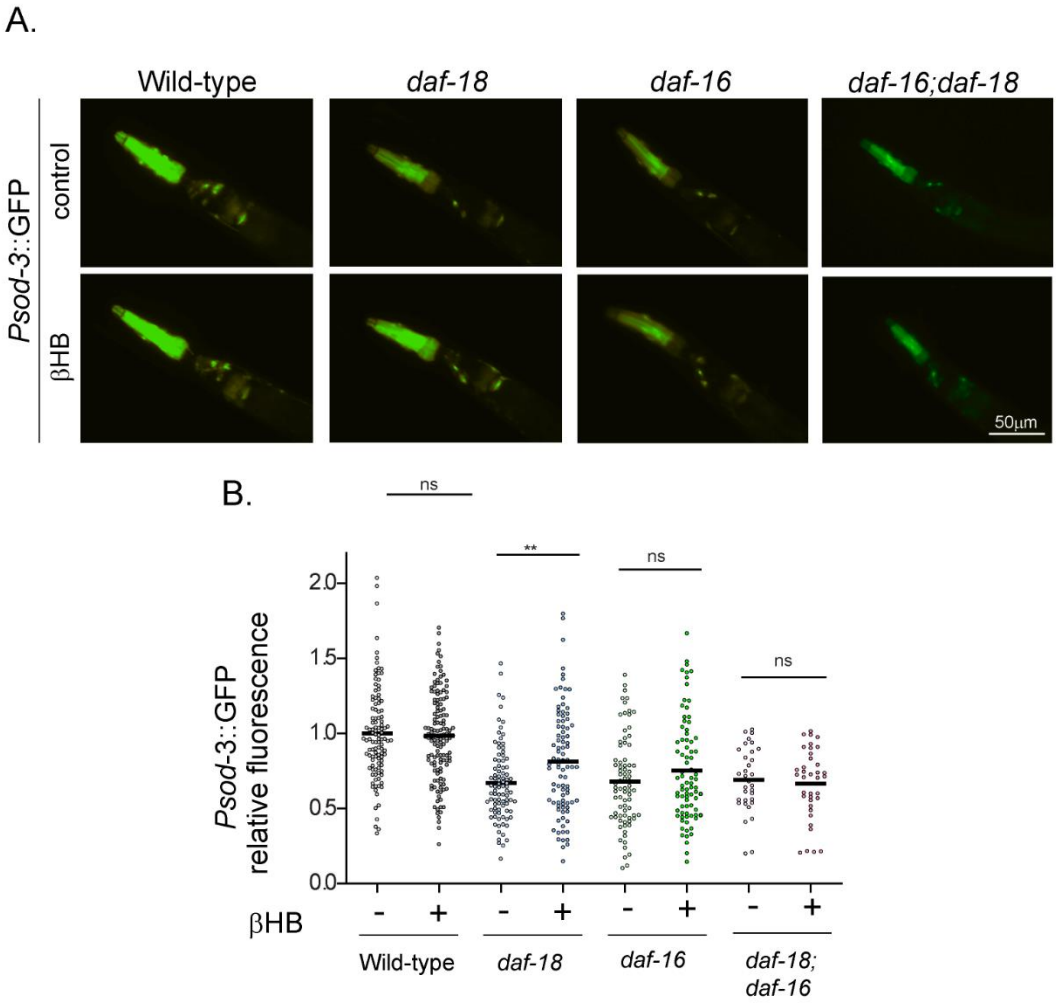

822

823 **Suppl. Figure 3. Exposure to βHB induces *sod-3* expression in *daf-18*, but not in *daf-16***
824 **mutants.**

825 A- Representative fluorescence images (20X magnification) of worms expressing *Psod-3::GFP*
826 in different genetic backgrounds (wild-type, *daf-18(ok480)*, *daf-16(mgDf50) and daf-18(ok480);*
827 *daf-16(mgDf50))* upon exposure to βHB (20mM). B- Corresponding quantification of the
828 fluorescence intensity per animal in the head. Scatter dot plot (line at the median) with the
829 relative expression of *Psod-3::GFP* normalized to naïve wild-type animals. Statistical

830 significance between conditions was determined by Kruskal-Wallis test (ns $p > 0.05$; ** $p \leq 0.01$;

831 **** $p \leq 0.0001$, n= 40-90).

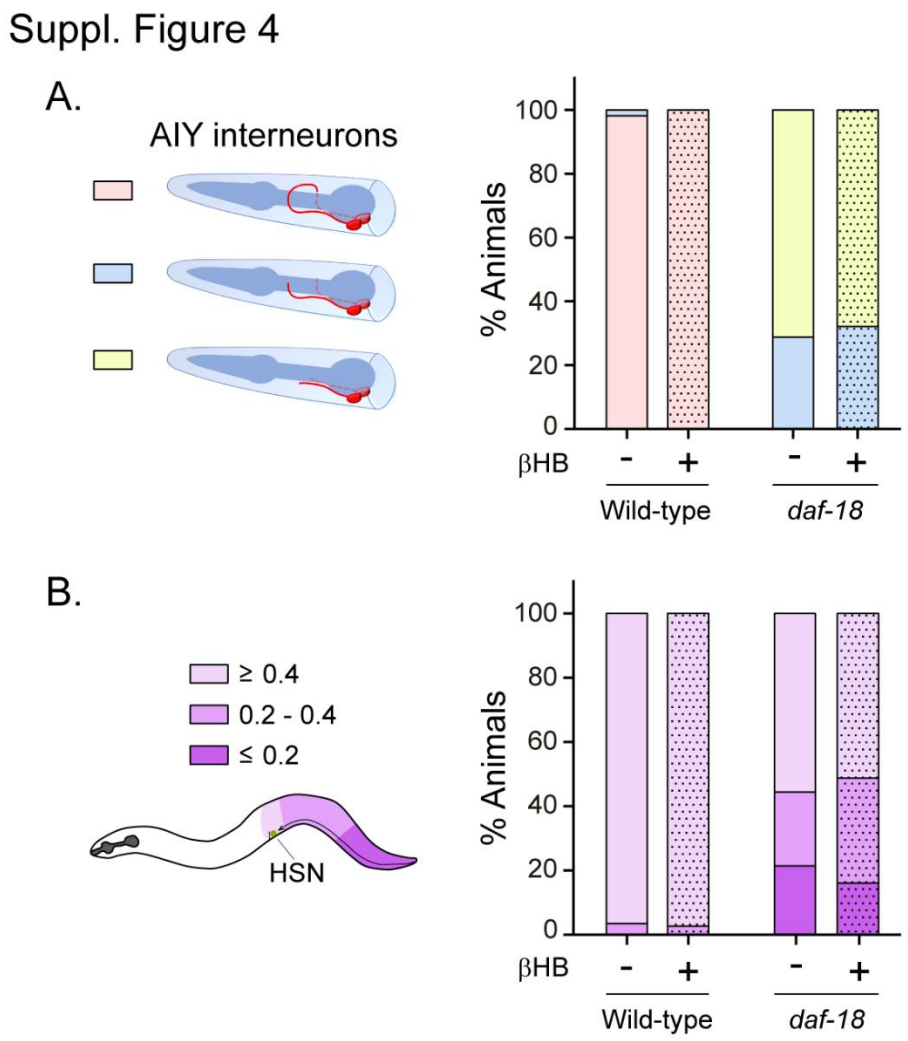

Suppl. Figure 4. βHB does not prevent neurodevelopmental defects in AIY and HSN neurons.

A- AIY processes were visualized in transgenic animals expressing cytoplasmic *GFP* in AIY neurons (*Pttx-3b::GFP*) in wild-type and *daf-18(ok480)* mutant backgrounds. AIY neuronal growth defects were quantified as described before (Christensen *et al*., 2011). Left: Scheme of AIY morphology and location in the nematode nerve ring. Blue, pharynx; red, AIY interneurons. Pink: wild-type AIY morphology. The two interneurons meet at the dorsal midline. Light blue and yellow: denote different levels of AIY neurite truncation. Right: Percentage of animals with truncated neurites in wild-type and *daf-18(ok480)* mutants under exposure (or not) to βHB (20

mM). B- HSN were visualized in transgenic animals expressing *GFP* in serotonergic neurons (*Ptph-1::GFP*) in wild-type and *daf-18(ok480)* mutant backgrounds. HSN under-migration defects were identified as described before (Kennedy et al., 2013). Left: Schematic representation of the HSN migratory route during embryogenesis and the corresponding location of the HSN (green circle) in a young adult animal. Only one of two bilaterally symmetric HSNs is illustrated. Colors show information about the position of HSNs: Light purple: complete migration (≥ 0.4), middle purple: intermediated migration (>0.2-<0.4), dark purple: unmigrated (≤0.2). Right: Quantification of the percentage of animals with different HSN migration positions (the most under-migrated neuron of each animal is considered). Bars represent the mean values of at least three independent experiments. Note that there is no significant effect with βHB treatment compared to controls.

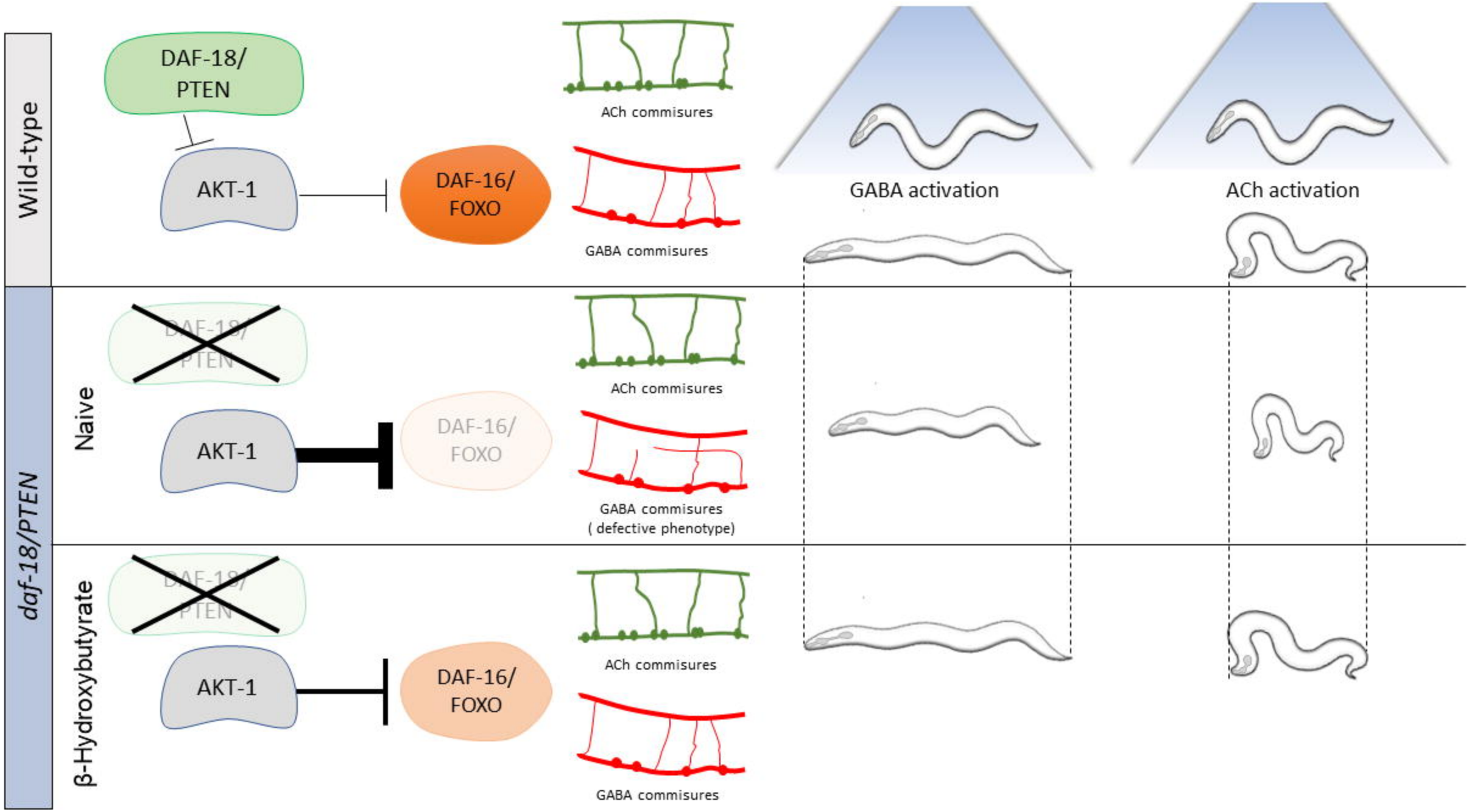
Wild-type
DAF-18/
PTEN
AKT-1
DAF-16/
FOXO
ACh commisures
GABA commisures
GABA activation
ACh activation
daf-18/PTEN
Naive
DAF-18/
PTEN
AKT-1
DAF-16/
FOXO
ACh commisures
GABA commisures
(defective phenotype)
β-Hydroxybutyrate
DAF-18/
PTEN
AKT-1
DAF-16/
FOXO
ACh commisures
GABA commisures